Experimental and analytical study of steel slit shear wall

Milad Khatamirad [a] and Hashem Shariatmadar[*]

Department of Civil Engineering, Ferdowsi University of Mashhad, Azadi Square, Iran

Abstract. A steel slit shear wall has vertical slits and when it is under lateral loads, the section between these slits has double-curvature deformation, and by forming a flexural plastic hinge at the end of the slit, it dissipates the energy on the structure. In this article, Experimental, numerical and analytical analyses are performed to study the effect of slit shape and edge stiffener on the behavior of steel slit shear wall. Seismic behavior of three models with different slit shapes and two models with different edge stiffener shapes are studied and compared. Hysteresis curves, energy dissipation, out of plane buckling, initial stiffness and strength are discussed and studied. The proposed slit shape reduces the initial stiffness, increases the strength and energy dissipation. Also, edge stiffener shape increases the initial stiffness significantly.

Keywords: steel slit shear wall; analytical analysis; energy dissipation; hysteresis curve

1. Introduction

Shear walls are considered one of the main lateral resisting members in buildings. A number of experimental and numerical studies have been conducted in recent years. Jayalekshmi and Chinmayi (2016) studied seismic analysis of shear wall buildings incorporating site-specific ground response. Parulekar *et al.* (2016) evaluated the seismic performance of mid-rise shear walls experimentally and numerically. Sabuncu *et al.* (2016) studied the static and dynamic stability of cracked multi-story steel frames. Dhar and Bhowmick (2016) estimated the seismic response of steel shear walls using nonlinear static methods. Rahmzadeh *et al.* (2016) studied the effect of stiffeners on steel plate shear wall systems. Vatansever and Berman (2015) studied analytical investigation of thin steel plate shear walls with screwed infill plate. Vatansever and Yardimci (2011) studied experimental investigation of thin steel plate shear walls with different infill-to-boundary frame connections.

The steel slit shear wall (slit wall) is a new promising lateral force resisting system. The most notable benefits of the system are its ductile behavior and its ability to dissipate energy. Mutō (1968) introduced concrete slit shear wall as an energy dissipating system. The wall has slits with equal distances at the middle of the wall height. The slits are created by cutting the concrete and reinforcement completely. The concrete slit shear wall has a higher ductility and a lower strength than the concrete shear wall. In small drift, the wall acts as a shear wall and restricts deformations. In large drift, the slits act as a series of flexural members and dissipate energy. The system was first used in a 36-story building in Japan and then in dozens of high-rise buildings. Although the walls increase the ductility, the number of walls increases due to the decrease in strength, and hence, the structures' weight increases and seismic lateral forces increase. In addition, reinforced concrete quickly collapses against cyclic plastic deformations. These two reasons prevented the widespread use of concrete shear walls (Muto *et al.* 1973).

Hitaka and Matsui (2003) studied the slit wall experimentally and numerically. They studied the effect of slit on a slit wall in 42 experimentally samples with a scale of 1 to 3. The parameters of the study were as follows: b/t (ratio of width to thickness of the link, α (ratio of length to thickness of the link), m (number of rows of the link) and the edge stiffener effect. Most samples deformed without the strength degradation to the drift of about 3%. They also found that samples with the b/t less than 20 have a stable cyclic behavior. In another part of the research, the effect of the width of the edge stiffener was studied on the slit wall behavior. The increase in the width of the edge stiffener slightly affected the stiffness and strength of the slit wall. However, its behavior was more stable after the out-of-plane buckling began. Hitaka and Matsui (2003) regarded the out-of-plane buckling of a slit wall as the main factor for strength degradation. According to the research results, three 7- to 19-storey buildings were designed and built in Japan.

Hitaka *et al.* (2007) studied the effect of the slit wall on the moment frame in two groups. The first group included three single-span one-floor frames and the second group included four single-span three-floor frames with a scale of 1 to 3. The walls were designed to tolerate 10 to 25% base shear and the moment frame tolerated the rest. Samples in the first group deformed to the drift 7% and those in the second group deformed to the drift 4% without any degradation of the strength and wall crack. They found that the effect of the wall on the frame stiffness is more than that

---
*Corresponding author, Associate Professor,
  E-mail: shariatmadar@um.ac.ir
[a] Ph.D. Candidate, E-mail: miladkhatami@ut.ac.ir

of the frame strength.

Jacobsen *et al.* (2010) studied the configuration of the links numerically. They modeled two samples named as modified samples and compared them with a normal sample (with links with constant length and distance) to study the effect of the links' length and their distance on the slit wall behavior. The results of the study showed that the behavior of the sample with different lengths of links does not significantly differ from a normal sample; however, samples with a variable distance between the links show a better behavior than the normal sample.

Cortes and Liu (2011) conducted two sets of tests on the slit wall (5 tests) and frame-slit wall (5 tests). In the first set of tests, the basic features of the slit wall were studied and in the second set, the interaction between frame and slit wall was studied. The strength, stiffness, stress distribution and failure modes were considered as the parameters of study in the first set, and they included beam-frame bending inertia moment, wall thickness, and the number of walls in a span and number of floors.

Most samples deformed to the drift 5% without any significant decrease (to the final strength 80%). The bending stiffness of the beams significantly affects the initial frame-wall stiffness. Also, the increase in the number of walls in a span does not significantly affect the frame-wall stiffness.

The most important difference between the samples in Cortes and Liu (2011) article and those in Hitaka and Matsui (2003) is that the shear frames tested by Cortes and Liu (2011) were designed to tolerate all base shear applied, and the shear frames tested by Hitaka and Matsui (2003) were designed to tolerate only 10 to 25% of the base shear.
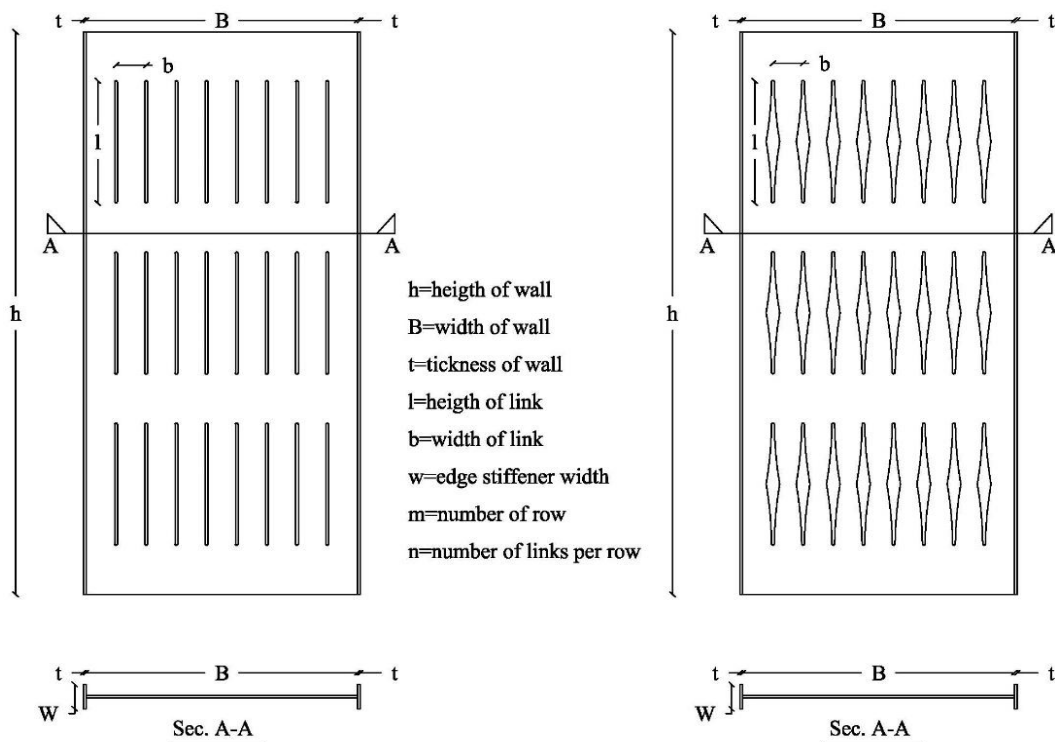
Also, the height to width ratio of the slit walls in the study by Cortes and Liu (2011) was about 2, while that in the study by Hitaka and Matsui (2003) was about 1 and the slit wall had filled the main part of the span.

According to the studies performed so far, the main purpose of the present article is to study the effect of slit shape and edge stiffener type on the strength, initial stiffness and energy dissipation of the slit wall analytically, numerically and experimentally. The obtained results suggest that the proposed slit shape reduces the initial stiffness and increases the strength and energy dissipation. Also, according to the study by Hitaka and Matsui (2003) on the width of the edge stiffener, the effect of the type of the edge stiffener is tested on the slit wall behavior in this article. The type of the edge stiffener increases the initial stiffness and strength of the slit wall.

2. Strength and stiffness of slit wall

In this section, the basic equations for stiffness and strength of the slit wall are presented. In Fig. 1, geometrical characteristics of a wall with normal and modified slits are indicated.

The ductile behavior of the slit wall depends on the geometrical characteristics of the slits. Hitaka and Matsui (2003) introduced three important parameters to control the ductile behavior of the slit wall: α, β and b/t. α is equal to l/b. This ratio ensures the flexural behavior of the links. The proposed value for α ranges from 2.5 to 5. β is ml/h. This ratio shows that a suitable part of the slit wall is composed of the slit. The proposed value for β ranges from 0.65 to

h=heigth of wall
B=width of wall
t=tickness of wall
l=heigth of link
b=width of link
w=edge stiffener width
m=number of row
n=number of links per row

(a) Geometrical characteristics of a slit wall with a normal slit   (b) Geometrical characteristics of a slit wall with a modified slit

Fig. 1 Geometrical characteristics of a slit wall

0.85. The third parameter controls the out-of-plane buckling of the links. Its proposed value ranges from 10 to 15.

The shear strength of the slit wall is obtained by the sum of the shear strength of the links and edge stiffeners. Hitaka and Matsui (2003) and Cortes and Liu (2011) presented the equations of the slit wall strength. Eq. (1) presents more accurate and complete equation of the wall's shear strength that is obtained based on analytical equations.

$$Q_u = \frac{F_y t}{2l}\left[(n-2)b^2 + \frac{8M_{Pst}}{F_y t}\right] \tag{1}$$

Where F_y is the steel yield stress, M_{Pst} is the plastic moment of the first and last link together with the stiffener, and other parameters are defined. Also, it is assumed that the thickness of the wall and edge stiffener is equal.

M_{Pst} differs based on the edge stiffener shape. If the edge stiffener is a sheet, the shear strength of a normal slit wall is obtained using Eqs. (2)-(3), and the shear strength of a modified slit wall is obtained using Eqs. (4)-(5). The equations of other edge stiffener shapes (channel and tube stiffeners) are more complex.

$$Q_u = \frac{F_y t}{2l}\left[nb^2 + 4bw + 4wt - 2w^2\right] \quad (\text{if} \quad w < b) \tag{2}$$

$$Q_u = \frac{F_y t}{2l}\left[nb^2 + 2bt + 2wt + 2b^2\right] \quad (\text{if} \quad w > b) \tag{3}$$

$$Q_u = \frac{F_y t}{2l}\left[4bw + 4wt - 2w^2\right] + F_y ta^2 (if w < b) \ (\text{if} \quad w < b) \tag{4}$$

$$Q_u = \frac{F_y t}{2l}\left[2bt + 2wt + 2b^2\right] + F_y ta^2 (if w > b) \quad (\text{if} \quad w > b) \tag{5}$$

Where w is the width of the edge stiffener and $a = \frac{b(x)}{2\sqrt{x}}$.

Due to the tendency of the sheet for out-of-plane buckling, the wall's buckling strength must be controlled to form plastic hinges at the end of the link before buckling occurs. Buckling can occur generally or in the links. The overall buckling of the wall is obtained using Eq. (6) based on the equation offered by Timoshenko and Gere (1961). When obtaining the buckling strength, the effect of the slits is neglected to prevent from complicating the equations.

$$Q_{LTB} = \left[\frac{4.013}{\left(\frac{h_{LTB}}{2}\right)^2}\right]\sqrt{EI_{panel}C} \tag{6}$$

I_{panel} is the inertia moment of the wall of edge stiffener around the weak axis, $C = GJ$ is the torsional constant that is obtained for the edge stiffener based on Eq. (7). G is the shear modulus and h_{LTB} is the height of the wall at the

distance between the center of the upper and lower torsions.

$$C = GJ = \left(\frac{Gt^3}{3}\right)(2w + B - 2t) \tag{7}$$

Hitaka and Matsui (2003) found that out-of-plane buckling of the links occurs simultaneously in a row. The out-of-plane buckling strength of the links is obtained by the product of the buckling strength of a link and the number of links in a row. The buckling strength of the links is obtained by Eq. (8) based on the equations by Timoshenko and Gere (1961).

$$Q_{LTB} = n\left[\frac{4.013}{\left(\frac{l}{2}\right)^2}\right]\sqrt{EI_{link}c} \tag{8}$$

I_{link} is the inertia moment of a link around the weak axis $(bt^3/12)$ and c is the torsional constant that is obtained by Eq. (9).

$$c = GJ = \left(\frac{Gbt^3}{3}\right)\left[1 - 0.63\left(\frac{t}{b}\right)\right] \tag{9}$$

The shear buckling strength of the wall must be also calculated to examine the out-of-plane buckling precisely. The shear buckling strength is obtained from Eq. (10) based on the equations by Timoshenko and Gere (1961).

$$Q_{Scr} = \frac{\pi^2 K_{cr} E}{12(1-v^2)}\left(\frac{t}{h}\right)^2 Bt \tag{10}$$

v is Poisson's ratio and K_{cr} is a parameter based on the type of loading and boundary conditions that is obtained from Eq. (11) based on the equations by Timoshenko and Gere (1961).

$$K_{cr} = 5.34 + 4\left(\frac{B}{h}\right)^2 \tag{11}$$

Another important parameter is the slit wall stiffness. The slit wall stiffness is obtained by the combination of the bending and shear stiffness of the links and the stiffness of the regions between the links. After calculating the stiffness of any link, the stiffness of the links in a row is added in parallel to each other and then the stiffness of any row is added to that of other rows in series. The normal slit wall stiffness is obtained by Eq. (12) and the modified slit wall stiffness is obtained by Eq. (13). The first part of the equation is the stiffness of the regions between the links, and the second part of the equation is the bending and shear stiffness of the middle links and the first and last links (taking the edge stiffener into account).

$$K = \frac{1}{\dfrac{k(h-ml)}{GBt} + \dfrac{m}{\dfrac{n-2}{\dfrac{k(\alpha,\beta)l^3}{Eb^3t} + \dfrac{kl}{Gbt}} + \dfrac{2}{\dfrac{k(\alpha,\beta)l^3}{12EI_{st}} + \dfrac{kl}{GA_{st}}}}} \tag{12}$$
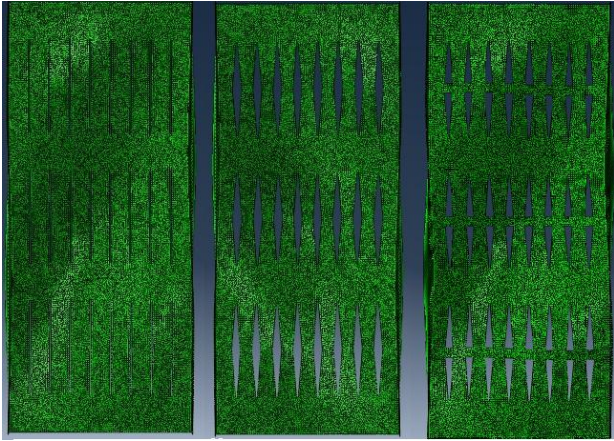
Fig. 2 Finite element model of slit walls

$$K = \cfrac{1}{\cfrac{k(h-ml)}{GBt} + \cfrac{m}{\cfrac{n-2}{\cfrac{2k(\alpha,\beta)\sqrt{(l/2)^3}}{Ea^3t} + \cfrac{2k\sqrt{l/2}}{Gat}} + \cfrac{2}{\cfrac{k(\alpha,\beta)}{K_{st}} + \cfrac{1}{K_{stshear}}}}} \quad (13)$$

K is the form factor of shear deformation that is 1.2 for a rectangular cross section. K_{st} is the bending stiffness, $K_{stshear}$ is the shear stiffness, I_{st} is the inertia moment and A_{st} is the area of the first and last links together with the stiffener. $K(\alpha, h/B)$ is the factor of bending stiffness reduction and it is obtained by Eq. (14). According to the investigations performed by Hitaka and Matsui (2003), the beginning and end parts of the links are not fixed and they rotate due to the stress concentration on the beginning and end parts of the slits and formation of plastic hinges in these regions. $K(\alpha, h/B)$ factor is used to take the effect of these rotations into account in the bending stiffness equation that is obtained by assuming fixed beginning and end parts.

$$K(\alpha, h/B) = \left(1 + \frac{1}{\alpha}\right)^{3\frac{h}{B}} \quad (14)$$

The power of Eq. (14) presented by Hitaka and Matsui (2003) is 3. According to the experimental results in this article, those presented by Cortes and Liu (2011) and those presented by Hitaka and Matsui (2003), the power $3\frac{h}{B}$ correlates very well.

3. Finite element analysis

The main purpose of this section is to present a reliable numerical model for simulating the slit wall behavior under cyclic loading. Using finite element model, stiffness and strength are studied in the slit wall. The slit wall is modeled by shell element (S4R) in Abaqus. S4R is a general four-point two-curvature element with reduced integration. Any point has 6 degrees of freedom: three translational degrees (U_x, U_y, U_z) and three rotational degrees (θ_x, θ_y, θ_z). The element can be used for thin and thick shells (Abaqus 2014). In Fig. 2, finite element models are shown.

The results of uniaxial testing are defined as material specifications in the software. One of the factors of strength degradation in the slit wall is stress concentration at the end of slits and crack development. Two main processes that damage soft metals are as follows: ductile damage due to nucleation, growth and coalescence of holes, and shear damage due to shear band localization (Shi *et al.* 2011). Both ductile and shear damages must be modeled correctly to model damage in Abaqus.

Also since one of the other main factors of the strength degradation of slit wall is out-of-plane buckling (Hitaka *et al.* 2007), it must be modeled correctly. The initial stiffness and slit wall strength are very high under in-plane lateral loads. However, the initial defects reduce the initial stiffness and strength significantly. For this purpose, buckling analysis must be first performed by Abaqus. In this article, after performing buckling analysis using Eigenvalue Method, and changing the input file of the software, a combination of all deformations from linear buckling modes is used by applying small factors as initial geometrical models of the slit wall in nonlinear buckling
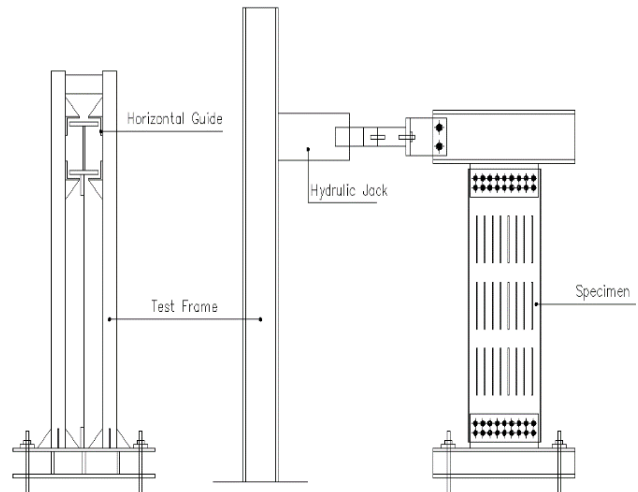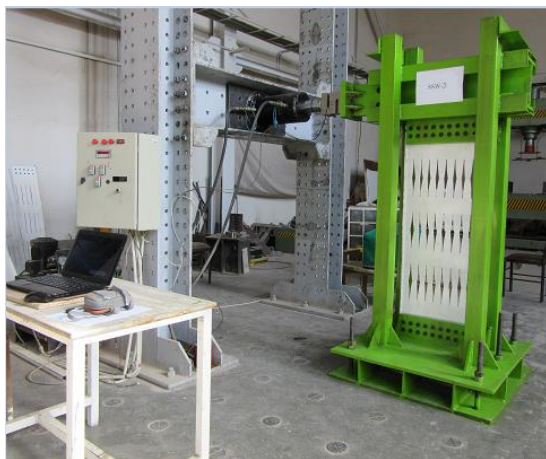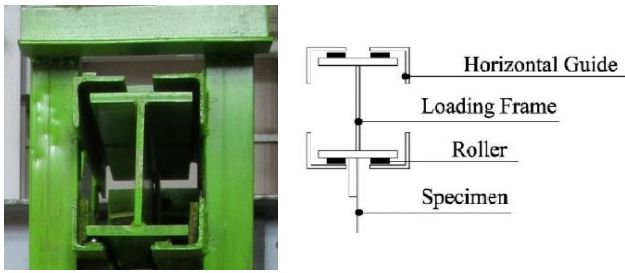

Fig. 3 Setup of experiment
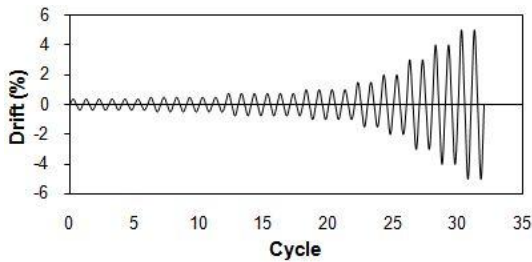
Fig. 4 Horizontal displacement system

Fig. 5 Loading pattern

analysis. This creates initial defects in the initial model that makes modeling closer to reality (Wang *et al.* 2015).

In Section 5, the results of finite element model are compared with those from experimental testing and analytical equations.

4. Experimental setup

The most important section of the present article is to perform experimental studies on five slit wall samples. The experiments are performed to study the behavior, stiffness, strength and hysteresis curve of the slit wall. The experiments are classified into two groups. In the first group, three tests are performed to study the effect of the slit shape on wall behavior, whereas in the second group, two tests are performed to study the effect of the edge stiffener on wall behavior. In Table 1, specifications of samples are presented briefly with a 1/3 scale. Also, Figs. 7-11 illustrate the slit walls. In this paper, the stiffness, strength, failure modes, dissipated energy, and ductility are the most important parameters that are studied. Then, the stiffness and strength of the test results are compared with those from the finite element modeling and analytical equations.

After preparing the samples according to the presented

specifications, the wall was loaded laterally by a jack with the capacity 300 KN. The loading was based on the displacement control.

In Fig. 3, the schematic diagram and actual setup of the experiment are presented.

Above the wall, there is a beam on which a force is exerted. Four angles are used according to Fig. 4 so that the beam only moves horizontally and it does not have any out-of-plane movement.

Also, two LVDTs are used to measure the horizontal displacement.

Above the wall, there is a beam on which a force is exerted. Four angles are used according to Fig. 4 so that the beam only moves horizontally and it does not have any out-of-plane movement.

Also, two LVDTs are used to measure the horizontal displacement.

Due to the damage development in the slit wall, cyclic loading must be used (Krawinkler 2009). To compare the different test results, ATC-24 code (1992) has introduced standard loading patterns. The loading pattern in Fig. 5 is used in this article.

5. Experimental results

Two most crucial failure modes are a- tearing which due to stress concentration and crack development at the end of the slit and *b*- lateral-torsional and shear buckling. It is vital to avoid or delay these failures until after the wall is reached its ultimate capacity. In Sections 5.1 and 5.2, a novel experimental method is proposed to significantly decrease the stress concentration and out of plane buckling.

5.1 Effect of slit shape on slit wall behavior

The concentration of stress at the end of the slit and development of crack eventually result in strength degradation in the slit wall. Strength degradation can be decreased by reducing the concentration in these regions and developing stress and strain distribution in links height.

Consider the link presented in Fig. 6(a) and its moment distribution in Fig. 6(b). As it is observed, moment distribution is linear along the element. At any section such as A-A section, the basis of plastic section, $Z(x)$ and normal stress in the outer fiber of the section before yielding, $\sigma(x)$ can be calculated using Eqs. (15)-(16).

$$Z(x) = \frac{tb^2(x)}{4} \qquad (15)$$

Table 1 Specifications of slit wall samples

Test sample	Slit	Edge stiffener	n	m	Link width (mm)	Link height (mm)	Wall height (mm)	Wall width (mm)	Thickness (mm)
SSW-1	Normal	Sheet	9	3	50	250	1450	500	5
SSW-2	Modified	Sheet	9	3	50	250	1450	500	5
SSW-3	Modified	Sheet	9	3	50	250	1450	500	5
SSW-4	Normal	Channel	9	3	50	250	1450	500	5
SSW-5	Normal	Tube	9	3	50	250	1450	500	5

(a) A link of the slit wall   (b) Moment distribution
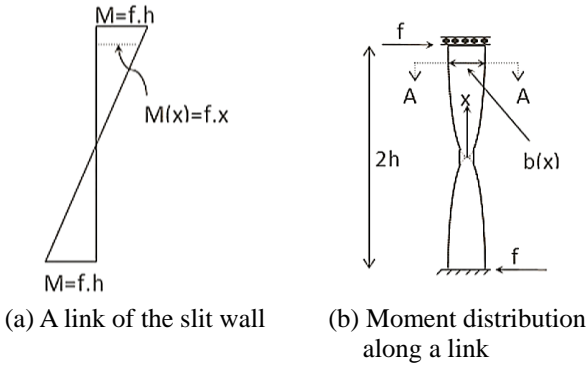   along a link

Fig. 6 A link of the slit wall and moment distribution
       along the link

$$\sigma(x) = \frac{M(x)}{Z(x)} = \frac{4fx}{tb^2(x)} \qquad (16)$$

The more uniform the stress distribution along a structural element, the higher its energy dissipation capacity will be. If for a link, the purpose is to create a uniform stress along the member during loading, the stress $\sigma(x)$, must be independent of the x value during loading. Therefore, if the section width, $b(x)$, is a factor of the square root of x, then we have

$$b(x) = 2a\sqrt{x} \qquad (17)$$

$$\sigma(x) = \frac{4fx}{4ta^2x} = \frac{f}{ta^2} \qquad (18)$$

It must be mentioned that a factor is not dimensionless and its dimension is the square root of length unit that must be taken into account in calculations. Since t and a are

constant for a link, Eq. (18) shows that if the section width, $b(x)$, is a factor of the square root of x, $\sigma(x)$ is independent of x. Hence, putting the yield stress value, σ_y, in Eq. (18), the load corresponding to the yield of the outer fiber of a link can be calculated. Also, the geometry ensures the yield growth in the whole section and simultaneously along the element according to Eq. (18). It should be noted that all the calculations and obtained results are based on the assumption that the link behavior is similar to Euler-Bernoulli beam and both ends of the link are fixed.

A normal slit wall and two proposed slit shapes are shown in Fig. 7. The purpose of the proposed slit shape is to reduce stress concentration at the end of slits and improve distribution of stress and strain in the height of links. In addition to using a different slit shape in the slit wall, the present article is different from slit walls in Cortes and Liu (2011), height of first and last parts of slit wall. It can be seen from Fig. 8 that height of the first and last parts of the slit wall has increased. In slit wall in Cortes and Liu (2011), it was not possible to extend the plastic hinge well and for this reason, slit walls were torn apart from this region.

In Fig. 9, hysteresis curves of the samples SSW-1, SSW-2 and SSW-3 are presented.

The test results and hysteresis curves in Fig. 9 show that out-of-plane buckling begins in the drift of 2.5%, and fine cracks develop at the end of slits in the drift of 3%. The slit wall deforms without any strength degradation to the drift of 5%. In all three walls after out-of-plane buckling, the change in distortion direction is observed due to the change in loading direction in the slit wall (Fig. 10) and pinching in the hysteresis curve. Also, the shape of the hysteresis curve is asymmetrical after out-of-plane buckling.

In Table 2, the initial stiffness values of the samples SSW-1, SSW-2 and SSW-3 are compared based on test results, analytical equations and numerical modeling. It can be deduced from the results that the initial stiffness of the
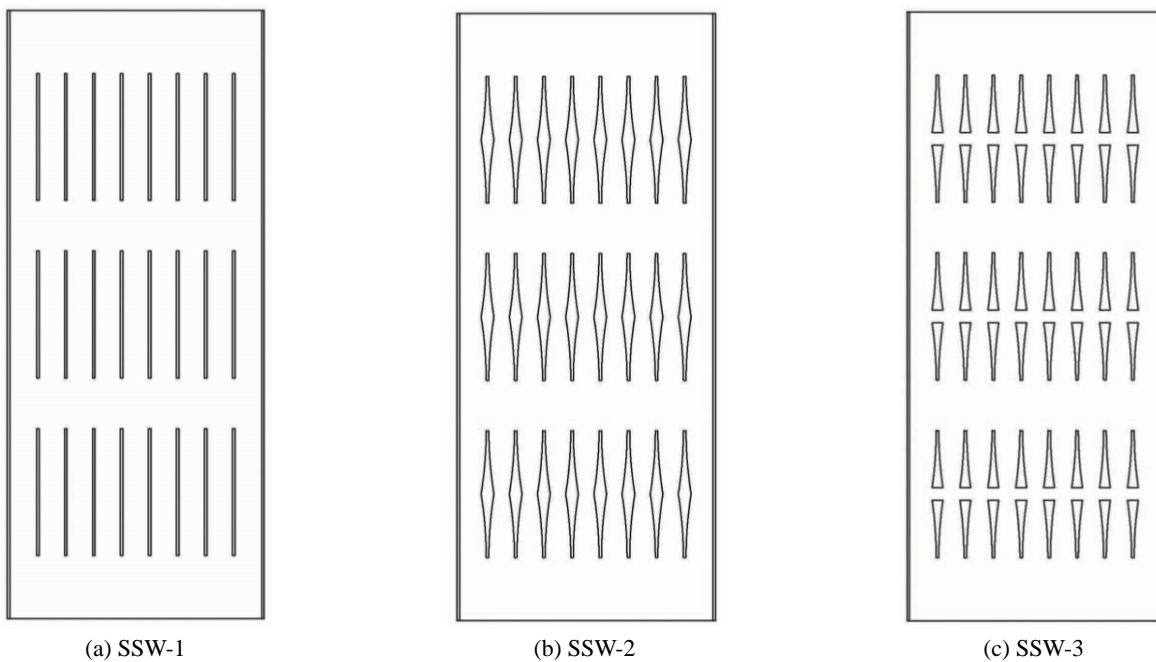

(a) SSW-1   (b) SSW-2   (c) SSW-3
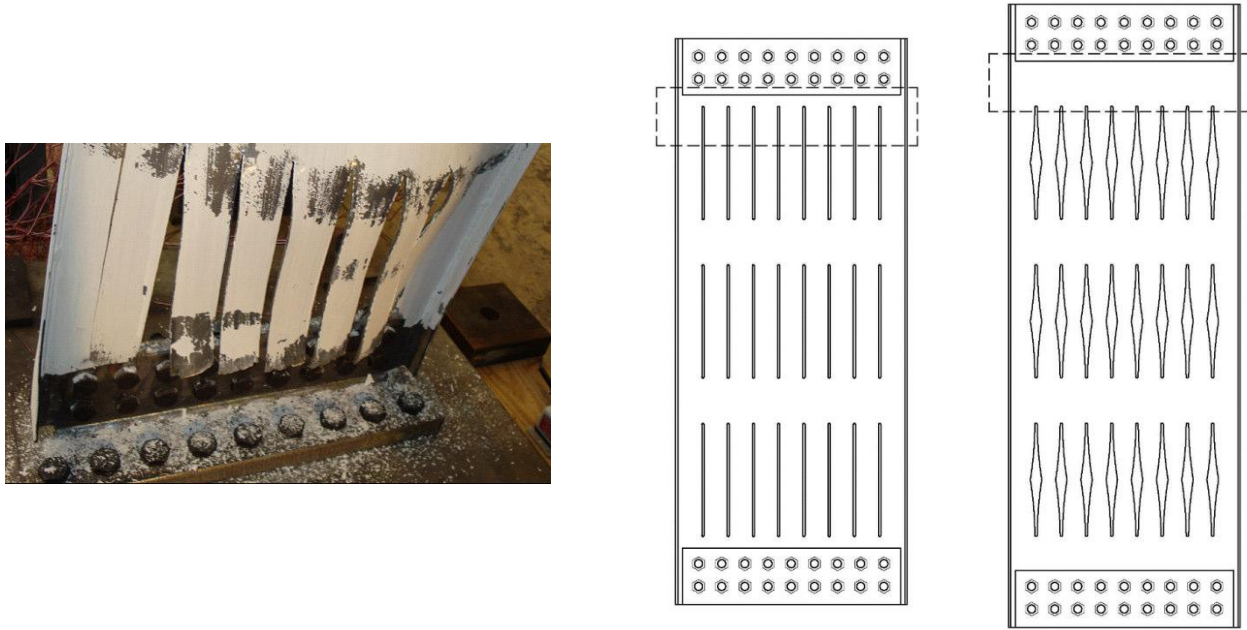
Fig. 7 A wall with normal and proposed slit shapes

Fig. 8 Difference between slit wall in this article and the one in Cortes and Liu article (2011)

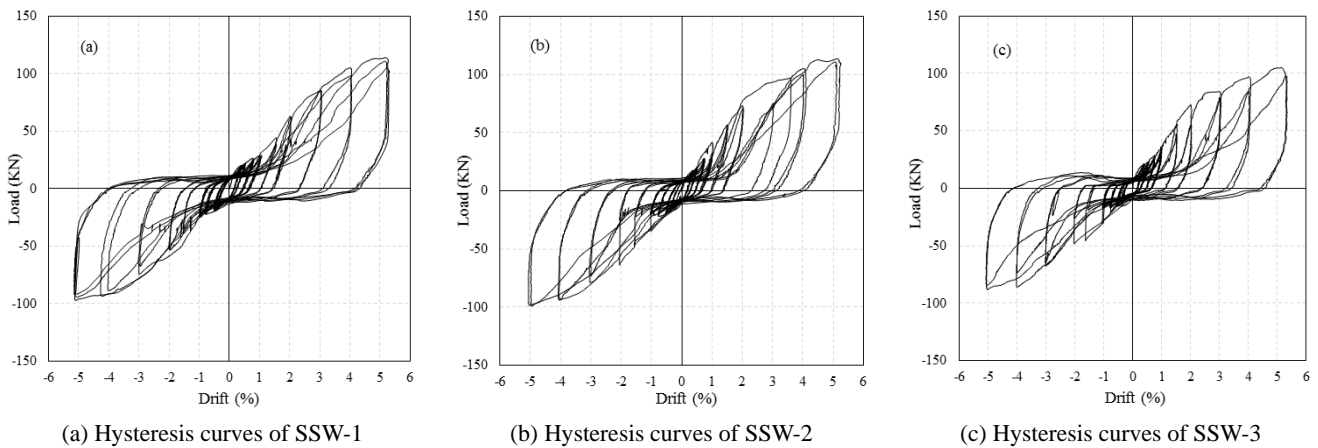(a) Hysteresis curves of SSW-1 (b) Hysteresis curves of SSW-2 (c) Hysteresis curves of SSW-3

Fig. 9 Hysteresis curves

Fig. 10 Change in distortion direction due to the change in loading direction in the slit wall SSW-2

wall SSW-2 has decreased by a factor of 5.7% compared to that of SSW-1, and the initial stiffness of the wall SSW-3 has increased by 17.8% compared to that of SSW-1. Also, analytical initial stiffness correlates with experimental initial stiffness very well.

Comparing three diagrams in Fig. 9, it is observed that the SSW-2 hysteresis curve is wider than the other two samples. In Table 3, the strength values of samples SSW-1, SSW-2 and SSW-3 are compared based on test results in different drifts. It is found that the strength of the wall SSW-2 has increased by 43.0% compared to that of SSW-1, while the strength of the wall SSW-3 has increased by 25.8% compared to that of SSW-1 in drift 1%.

Overall, yielding at the end of the links begins in the drift of 0.2% and complete in the drift of 2.5%, so the experimental strength of the slit wall is measured at drift of 2.5% (Table 4). The strength of slit wall increases after the drift 2.5% because of forming tension strips.

In Table 4, the strength values of samples SSW-1, SSW-2 and SSW-3 are compared based on the test results,

Table 2 Comparison of initial stiffness of the samples SSW-1, SSW-2 and SSW-3

Test sample	Experimental initial stiffness (KN/mm)	Analytical initial stiffness (KN/mm)	Difference (%)	Modeling initial stiffness (KN/mm)	Difference (%)
SSW-1	7.06	6.96	-1.5	8.25	16.9
SSW-2	6.68	6.47	-3.2	7.37	10.3
SSW-3	8.32	8.11	-2.6	9.45	13.6

Table 4 Comparison of strength of the samples SSW-1, SSW-2 and SSW-3

Test sample	Experimental strength (KN)	Analytical strength\ (KN)	Difference (%)	Modeling strength (KN)	Difference (%)
SSW-1	77.17	68.40	12.8	72.30	6.7
SSW-2	86.82	68.40	26.9	78.70	10.3
SSW-3	82.65	76.30	8.3	89.40	-8.2

Table 3 Comparison of experimental strength of the samples SSW-1, SSW-2 and SSW-3 in different drift

Drift (%)	Experimental strength (KN)				
	SSW-1	SSW-2	Difference (%)	SSW-3	Difference (%)
1	29.10	41.62	43.0	36.61	25.8
1.5	43.48	56.19	29.2	54.53	25.4
2	62.88	73.09	16.2	72.53	15.3
2.5	77.17	86.82	12.5	82.65	7.1

Table 5 Comparison of initial stiffness of the samples SSW-1, SSW-4 and SSW-5

Test sample	Experimental initial stiffness (KN/mm)	Analytical initial stiffness (KN/mm)	Difference (%)	Modeling initial stiffness (KN/mm)	Difference (%)
SSW-1	7.06	6.96	-1.4	8.25	16.9
SSW-4	9.79	9.65	-1.5	10.65	8.8
SSW-5	9.04	9.08	0.5	10.13	12.1

analytical equations and numerical modeling. It is clear from the results that the strength of the wall SSW-2 has increased by 12.5% compared to that of SSW-1, and the strength of the wall SSW-3 has increased by 7.1% compared to that of SSW-1 due to expansion of plastic zone in the height of links.

According to the research by Cortes and Liu (2011) and Hitaka and Matsui (2003), dimensional properties of the sheet and number of slits affect the strength, initial stiffness and energy dissipation of the slit wall. It can be observed from the results in Tables 2~4 and Fig. 9 that the slit shape also affects the strength and initial stiffness of the slit wall.

5.2 Effect of edge stiffener on slit wall behavior

Out-of-plane buckling is another factor of strength degradation that can occur for links or the whole wall. Out-of-plane buckling of a slit wall must be controlled in order that the plastic hinge develops at the end of slits. One way to reduce the out-of-plane buckling is to use edge stiffener (Hitaka *et al*. 2007). Hitaka and Matsui (2003) studied the effect of edge stiffener width on the initial stiffness, strength and shape of hysteresis curve. The width of edge stiffener
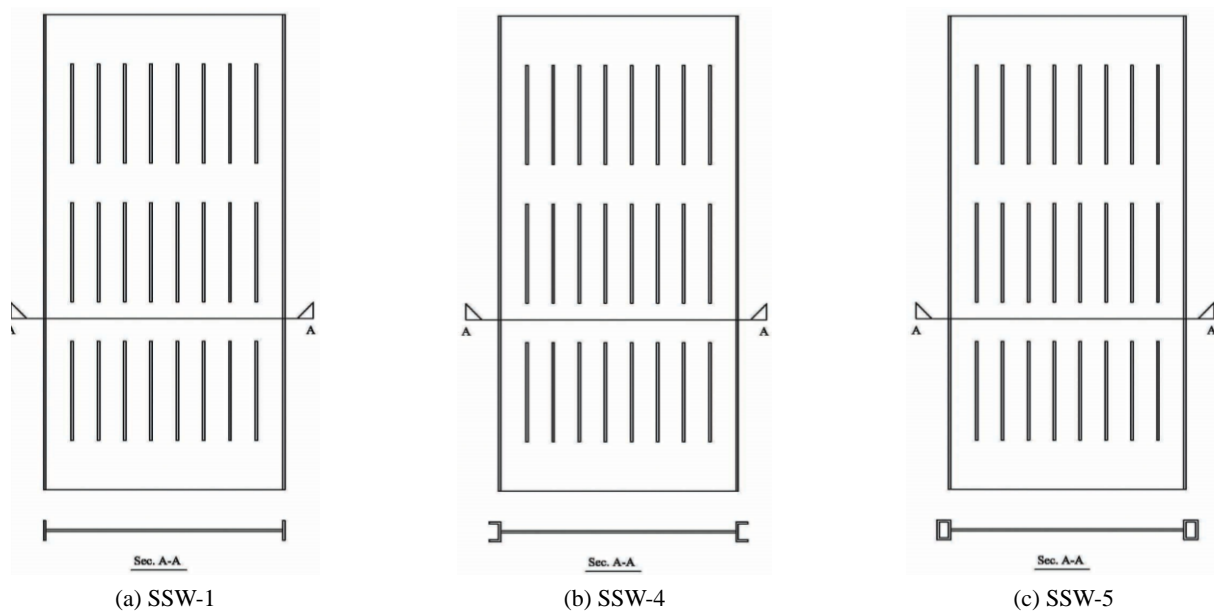

(a) SSW-1	(b) SSW-4	(c) SSW-5

Fig. 11 Slit walls with different edge stiffeners

(a) Hysteresis curve of the sample SSW-4

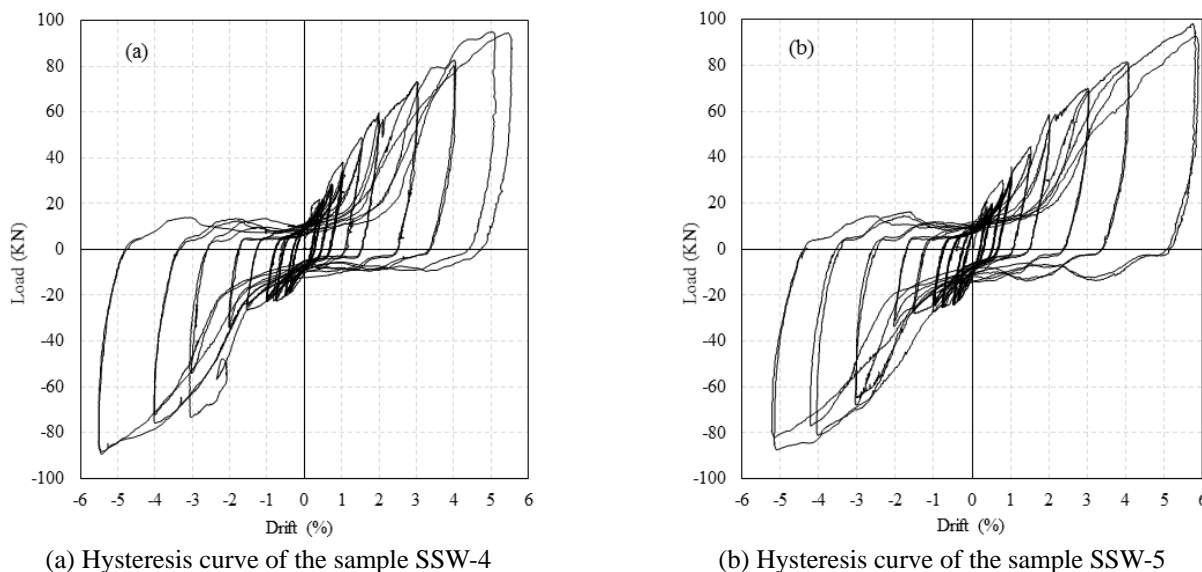(b) Hysteresis curve of the sample SSW-5

Fig. 12 Hysteresis curve

slightly increases the initial stiffness and strength and improves the hysteresis curve shape. In this article, the effect of the edge stiffener type is studied instead of increasing the width of the edge stiffener.

In Fig. 11, three slit walls are shown with different edge stiffeners to study the effect of the edge stiffener type on the slit wall behavior.

In Fig. 12, hysteresis curves of the samples SSW-4 and SSW-5 are shown.

The test results and hysteresis curves in Fig. 12 show that the out-of-plane buckling begins in the drift 4%, and fine cracks develop at the beginning and end of slits in the drift 3%. The slit wall deforms without any strength degradation to the drift 5%.

In Table 5, the initial stiffness values of the samples SSW-1, SSW-4 and SSW-5 are compared based on the test results, analytical equations and numerical modeling. It can be clearly seen that the initial stiffness of the wall SSW-4 has increased by 38.7% compared to that of SSW-1, and the initial stiffness of the wall SSW-5 has increased by 28.0% compared to that of SSW-1. Also, analytical initial stiffness correlates with experimental initial stiffness.

In Table 6, the strength values of the samples SSW-1, SSW-4 and SSW-5 are compared based on the test results in different drift. It can be concluded from the results that the strength of the wall SSW-4 has increased by 29.7% compared to that of SSW-1, and the strength of the wall SSW-5 has increased by 4.6% compared to that of SSW-1

Table 6 Comparison of experimental strength of the samples SSW-1, SSW-4 and SSW-5 in different drift

Drift (%)	Experimental strength (KN)				
	SSW-1	SSW-4	Difference (%)	SSW-5	Difference (%)
1	29.10	37.73	29.7	30.44	4.6
1.5	43.48	48.58	11.7	44.41	2.1
2	62.88	56.38	-11.5	58.6	-7.3
2.5	77.17	63.99	-20.6	62.55	-23.4

Table 7 Comparison of strength of the samples SSW-1, SSW-4 and SSW-5

Test sample	Experimental strength (KN)	Analytical strength (KN)	Difference (%)	Modeling strength (KN)	Difference (%)
SSW-1	77.17	68.40	12.8	72.30	6.7
SSW-4	63.99	68.40	-6.9	78.70	-23
SSW-5	62.55	68.40	-9.4	76.20	-21.8

in drift 1%.

In Table 7, the strength values of the samples SSW-1, SSW-4 and SSW-5 are compared based on the test results, analytical equations and numerical modeling. Accordingly, the strength of the wall SSW-4 has decreased by 20.6% compared to that of SSW-1, and the strength of the wall SSW-5 has decreased by 23.4% compared to that of SSW-1.

Based on the experimental results, the edge stiffener type increases the initial stiffness.

5.3 Comparison of energy dissipation capacity

Due to out-of-plane buckling in steel wall, pinching phenomenon occurs in the hysteresis curve of the wall that affects energy dissipation capacity. Energy dissipation factor is a parameter to show the level of energy dissipation. The energy dissipation factor is calculated based on Eq. (19) (Wang *et al.* 2015). $S_{(ABC)}$ and $S_{(CDA)}$ are areas of the upper and lower halves of the hysteresis curve, and $S_{(OBE)}$ and $S_{(ODF)}$ are areas of the triangular parts shown in Fig. 13.

$$E_P = \frac{S_{(ABC+CDA)}}{S_{(OBE+ODF)}} \tag{19}$$

Energy dissipation factor is shown in Fig. 14 and total energy dissipation is shown for the walls SSW-1, SSW-2,
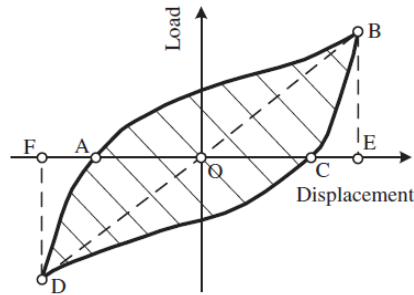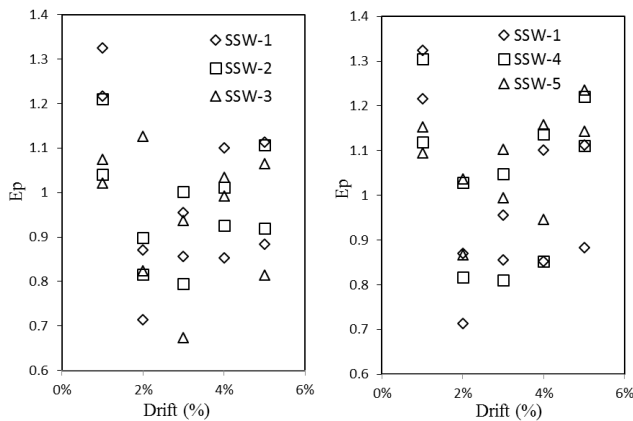
Fig. 13 Energy dissipation factor calculation method

(a) Comparison of the energy dissipation factor of the walls SSW-1, SSW-2, SSW-3

(b) Comparison of the energy dissipation factor of the walls SSW-1, SSW-4, SSW-5

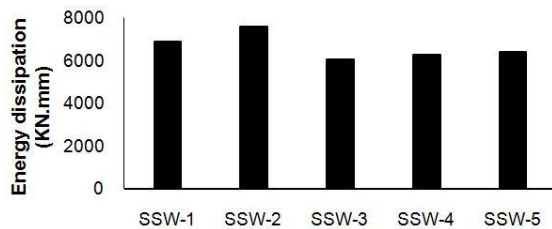Fig. 14 Comparison of the energy dissipation factor

Fig. 15 Comparison of the total energy dissipation of the walls SSW-1, SSW-2, SSW-3, SSW-4 and SSW-5

SSW-3, SSW-4 and SSW-5 in Fig. 15. According to Fig. 14, energy dissipation capacity decreases as the loading cycle repeats in a similar displacement.

Similarly, Fig. 15 shows that the change in slit shape and edge stiffener affects energy dissipation capacity. The energy dissipation of the wall SSW-2 has increased 10.2% compared to that of SSW-1 and the energy dissipation of another slit walls has decrease compared to that of SSW-1.

6. Conclusions

In this paper, two groups of slit walls were proposed, modeled and analyzed with different details to study the effect of slit shape and edge stiffener. The most important parameters of the study were initial stiffness, strength and

dissipated energy. Tearing at the end of the slit and buckling are the most crucial failure modes. It was observed from the results that slit shape and edge stiffener are the key parameters that affect the slit wall behavior. The proposed slit shape decreased stress concentration and edge stiffener decreased buckling .The results showed that the proposed slit shape in the wall SSW-2 decreased the initial stiffness of the slit wall by 5.7% and increased the strength by 12.5%. The proposed slit shape in the wall SSW-3 increased the initial stiffness of the slit wall by 17.8% and increased the strength by 7.1%. Also, slit shape developed stress distribution and expanded plastic zone in the height of links and increased energy dissipation. Furthermore, the type of edge stiffener decreased the out-of-plane buckling of the wall and increased the initial stiffness by 38.7% and 28.0% for the wall SSW-4 and SSW-5, respectively. The results indicated that the strength degradation did not occur up to drift of 5%. It should be noted that analytical initial stiffness correlated with Experimental initial stiffness very well. Finally, less than 13% mismatch was found between analytical strength and experimental strength except for SSW-2.

References

ATC-24 (1992), Guidelines for cyclic seismic testing of components of steel structures; ATC-24, Redwood City, CA, USA.

Abaqus, V.6.14 (2014), 6.14 Documentation; Dassault Systemes Simulia Corporation.

Cortes, G. and Liu, J. (2011), "Experimental evaluation of steel slit panel–frames for seismic resistance", *J. Constr. Steel Res.*, **67**(2), 181-191.

Dhar, M.M. and Bhowmick, A.K. (2016), "Seismic response estimation of steel plate shear walls using nonlinear static methods", *Steel Compos. Struct., Int. J.*, **20**(4), 777-799.

Hitaka, T. and Matsui, C. (2003), "Experimental study on steel shear wall with slits", *J. Struct. Eng., Int. J.*, **129**(5), 586-595.

Hitaka, T., Matsui, C. and Sakai, J.I. (2007), "Cyclic tests on steel and concrete-filled tube frames with Slit Walls", *Earthq. Eng. Struct. Dyn.*, **36**(6), 707-727.

Jacobsen, A., Hitaka, T. and Nakashima, M. (2010), "Online test of building frame with slit-wall dampers capable of condition assessment", *J. Constr. Steel Res.*, **66**(11), 1320-1329.

Jayalekshmi, B. and Chinmayi, H. (2016), "Seismic analysis of shear wall buildings incorporating site specific ground response", *Struct. Eng. Mech., Int. J.*, **60**(3), 433-453.

Krawinkler, H. (2009), "Loading histories for cyclic tests in support of performance assessment of structural components", *The 3rd International Conference on Advances in Experimental Structural Engineering*, San Francisco, CA, USA, October.

Mutō, K. (1968), *Earthquake Resistant Design of 36-storied Kasumigaseki Building*, Muto Institute of Structural Mechanics.

Muto, K., Ohmori, N. and Takahashi, T. (1973), "A study on reinforced concrete slitted shear walls for high-rise buildings", *Proceedings of the 5th World Conference on Earthquake Engineering*, Rome, Italy, June.

Parulekar, Y., Reddy, G., Singh, R., Gopalkrishnan, N. and Ramarao, G. (2016), "Seismic performance evaluation of mid-rise shear walls: Experiments and analysis", *Struct. Eng. Mech., Int. J.*, **59**(2), 291-312.

Rahmzadeh, A., Ghassemieh, M., Park, Y. and Abolmaali, A. (2016), "Effect of stiffeners on steel plate shear wall systems", *Steel Compos. Struct., Int. J.*, **20**(3), 545-569.

Sabuncu, M., Ozturk, H. and Yashar, A. (2016), "Static and dynamic stability of cracked multi-storey steel frames", *Struct. Eng. Mech., Int. J.*, **58**(1), 103-119.

Shi, Y., Wang, M. and Wang, Y. (2011), "Experimental and constitutive model study of structural steel under cyclic loading", *J. Constr. Steel Res.*, **67**(8), 1185-1197.

Timoshenko, S.P. and Gere, J.M. (1961), *Theory of Elastic Stability 1961*, McGrawHill-Kogakusha Ltd., Tokyo, Japan, 109 p.

Vatansever, C. and Berman, J.W. (2015), "Analytical investigation of thin steel plate shear walls with screwed infill plate", *Steel Compos. Struct., Int. J.*, **19**(5), 1145-1165.

Vatansever, C. and Yardimci, N. (2011), "Experimental investigation of thin steel plate shear walls with different infill-to-boundary frame connections", *Steel Compos. Struct., Int. J.*, **11**(3), 251-271.

Wang, M., Yang, W., Shi, Y. and Xu, J. (2015), "Seismic behaviors of steel plate shear wall structures with construction details and materials", *J. Constr. Steel Res.*, **107**(4), 194-210.

CC